Contents list available at IJRED website

Int. Journal of Renewable Energy Development (IJRED)

Journal homepage: http://ejournal.undip.ac.id/index.php/ijred

Thermal Decomposition and Kinetic Studies of Pyrolysis of *Spirulina platensis* Residue

Siti Jamilatun[a,b], Budhijanto[b], Rochmadi[b] and Arief Budiman[b,c,*]

[a]*Chemical Engineering Department, Ahmad Dahlan University, Jl. Kapas 9, Yogyakarta 55166, Indonesia*

[b] *Chemical Engineering Department, Gadjah Mada University, Jl. Grafika 2, Yogyakarta 55284, Indonesia*

[c]*Center for Energy Studies, Gadjah Mada University, Sekip K1A, Yogyakarta 55281, Indonesia*

ABSTRACT. Analysis of thermal decomposition and pyrolisis reaction kinetics of *Spirulina platensis* residue (SPR) was performed using Thermogravimetric Analyzer. Thermal decomposition was conducted with the heating rate of 10, 20, 30, 40 and 50°C/min from 30 to 1000°C. Thermogravimetric (TG), Differential Thermal Gravimetric (DTG), and Differential Thermal Analysis (DTA) curves were then obtained. Each of the curves was divided into 3 stages. In Stage I, water vapor was released in endothermic condition. Pyrolysis occurred in exothermic condition in Stage II, which was divided into two zones according to the weight loss rate, namely zone 1 and zone 2. It was found that gasification occurred in Stage III in endothermic condition. The heat requirement and heat release on thermal decomposition of SPR are described by DTA curve, where 3 peaks were obtained for heating rate 10, 20 and 30°C/min and 2 peaks for 40 and 50°C/min, all peaks present in Zone 2. As for the DTG curve, 2 peaks were obtained in Zone 1 for similar heating rates variation. On the other hand, thermal decomposition of proteins and carbohydrates is indicated by the presence of peaks on the DTG curve, where lignin decomposition do not occur due to the low lipid content of SPR (0.01wt%). The experiment results and calculations using one-step global model successfully showed that the activation energy (Ea) for the heating rate of 10, 20, 30, 40 and 50°C/min for zone 1 were 35.455, 41.102, 45.702, 47.892 and 47.562 KJ/mol, respectively, and for zone 2 were 0.0001428, 0.0001240, 0.0000179, 0.0000100 and 0.0000096 KJ/mol, respectively.

Keywords: *Spirulina platensis* residue (SPR), Pyrolysis, Thermal decomposition, Peak, Activation energy.

Article History: Received June 15th 2017; Received in revised form August 12th 2017; Accepted August 20th 2017; Available online
How to Cite This Article: Jamilatun, S., Budhijanto, Rochmadi, and Budiman, A. (2017) Thermal Decomposition and Kinetic Studies of Pyrolysis of *Spirulina platensis* Residue, International Journal of Renewable Energy Development 6(3), 193-201.
https://doi.org/10.14710/ijred.6.3.193-201

1. Introduction

The source of energy derived from crop and noncrop plants of the first and second generations of biomass not only competes with feedstock but also requires a large cultivation area (Chaiwong *et al.* 2013; Dragone *et al.* 2010). This has put the interests in the third generation of biomass as the alternative source of energy, including microalgae, which are believed to be the future energy source. With an efficient land for cultivation, it is possible to produce 40 – 80 ton of dry microalgae per hectare per annum (Wijffels, 2010). In addition, microalgae can grow in open pond as well as wastewater with a high CO_2 requirement (Hadiyanto *et al.* 2012) hence its cultivation can be employed as an alternative to rapidly reduce the greenhouse gasses emission from the proliferating industrial operation (Hadiyanto *et al.* 2013; Sunarno *et al.* 2017).

Energy source from microalgae which is processed into biodiesel usually contains lipid in a high concentration of lipids, such as *Scenedesmus dimorphus* (16-40 wt%), *Chlorella vulgaris* (14-49.5 wt%), *Prymnesium parvum* (22-39 wt%), and *Nannochloropsis oceanica* (24.8 wt%) (Suganya *et al.* 2016). After the lipid content is extracted, the solid waste with a very low lipid content (0.01 wt%) is obtained. An inappropriate disposal of this waste will contaminate the environment. Moreover, the waste cannot be used as animal feed due to its remaining methanol content after extraction (Chisti 2008). The waste also still contains protein and carbohydrate at an

* Corresponding author: abudiman@ugm.ac.id

adequately high level (Ceylan *et al.* 2014), therefore exhibiting a great potential to process thermochemically into a new source of energy (Ananda *et al.* 2016).

The lipid content in the solid waste of microalgae extraction, such as *Chlorella vulgaris* residue (5.71 wt. %), *Spirulina platensis* residue (0.01 wt %), *Chlorella sorokiniana* CY1 residue (9.9 wt. %), and *Nannochloropsis oceanica* residue is notably low. On the other hand, their high protein and carbohydrate content offers an attractive potential as a raw material of bio-oil (Chen et al., 2015). Bio-oil has attracted immense attractions due to its high calorific value such as from *Chlorella vulgaris* residue (24.57−35.10 MJ/kg), *Spirulina platensis* residue (20.46 – 33.62 MJ/kg), *Chlorella sorokiniana* CY1 residue (20.24 MJ/kg), and *Nannochloropsis oceanica* residue (32.33−39 MJ/kg) (Chen *et al.* 2015). As a comparison, these calorific values are higher than bio-oil produced from lignocellulose such as coconut shell (21.28 MJ/kg) and sugarcane bagasse (El-Sayed *et al.* 2014).

So far, many studies have been done to produce bio-oil from microalgae using various technologies. Among them, thermochemistry by pyrolysis is simpler and can be performed at atmospheric pressure. Moreover, unlike liquefaction, pyrolysis does not require solvents (Lia *et al.* 2013; Widiyannita *et al.* 2015). The bio-oil production in industrial scale needs to be evaluated in regards to the process feasibility, especially for reactor design, hence requiring kinetic data (Pratama *et al.* 2014; Ojolo *et al.* 2013; Daniyanto *et al.* 2016) and decomposition characteristics (Hu *et al.* 2015). Previously, Agrawal and Chakraborty (2013) reported that in the pyrolysis of *Chlorella vulgaris*, the activation energy of protein and carbohydrate decomposition in Stage II in Zone I is 51 kJ/kg, lower than the activation energy of lipid (64 kJ/kg) that occurs in Zone 2.

Thermal Gravimetric (TG), Differential Thermal Gravimetric (DTG), and Differential Thermal Analysis (DTA) methods are very important in investigating the kinetics and thermal decomposition characteristics of biomass in a thermochemical conversion process (Wang *et al.* 2016). These methods have a high accuracy to study the degradation conditions in kinetic regime (Li *et al.* 2016). The decomposition mechanism and kinetic model are predicted and tested with data obtained from experiments (Wicakso *et al.* 2017). Therefore, this study aims to investigate the thermal decomposition characteristics and kinetics in pyrolysis process of *Spirulina platensis* residue (SPR) using a distribution model of activation energy in various heating rates with the one-step global model.

2. Materials and Methods

2.1 Materials

The raw material used in this study was solid waste from SPR which was dried using a microwave at 60°C until a constant weight was obtained. The dried solid was then extruded until a homogenous size of 125 µm. Ultimate analysis, protein, lipid, and carbohydrate content analysis, and calculation of the caloric value of the waste from SPR were performed in Research and Development of Energy and Mineral Resources, Center for Research and Development of Mineral and Coal Technology, Bandung.

2.2 Experimental methods

Thermal decomposition and pyrolisis kinetics of SPR were studied by Thermogravimetric Analyzer using Perkin Elmer Pyric Diamond TG-DTA. The SPR sample for each experiment, 3.536 – 11.933 mg in weight, was fed into alumina crucible which was operated in non-isothermal condition. Heating was done in a range of 30 – 1000°C with the heating rate of 10, 20, 30, 40 and 50°C/min while exhaled with pure nitrogen gas at a rate of 20 mL/min. The temperature was kept constant for 5 minutes when reached 120 and 600°C to ensure complete water vaporisation and pyrolisis.

2.3 Kinetic modeling

The proposed kinetic model was the one-step global model, assuming that the weight change of the sample was observable. This model also assumes pyrolysis as a one-step order 1 reaction, where organic fuel decomposes into volatile matter and char with a constant char production (Equation 1) (Prakash and Karunanithi 2008).

$$\text{Biomass} \rightarrow \text{Volatile Matter} + \text{Char} \quad \textbf{(1)}$$

The sample was pyrolyzed with Thermogravimetric Analyzer in non-isothermal condition. The weight change of the sample was noted. The change of conversion and degradation in regards to time, dX/dt, depends on the rate of reaction constants which are influenced by temperature [k(T)] and conversion [f(X)], expressed as:

$$\frac{dX}{dt} = k(T).f(X) \quad \textbf{(2)}$$

where:

- X is conversion,
- t is time (minute),
- T is temperature (K).

The rate of reaction constants, k, are calculated using the Arrhenius equation:

$$k = A.\exp\left(\frac{-Ea}{RT}\right) \quad \textbf{(3)}$$

where:

- A is Arrhenius factor,
- Ea is activation energy,

- R is universal gas constant (J/mole.K).

The function f(X) is expressed as:

$$f(X) = (1 - X)^n \quad (4)$$

where n is the order of reaction, in this case, is assumed to be one. The SPR conversion (X) is calculated with Ojolo et al. (2013):

$$X = \frac{m_0 - m_t}{m_t - m_\sim} \quad (5)$$

where:

- m_o is the initial weight of SPR,
- m_t is the weight of SPR at time t,
- m_∞ is the final weight of SPR at the end of the reaction.

Combining Equation (1–4) results in:

$$\frac{dX}{dt} = A.\exp\left(\frac{-Ea}{RT}\right)(1 - X)^n \quad (6)$$

$$T = T_0 + \beta(t) \quad (7)$$

$$\beta = \frac{dT}{dt} \quad (8)$$

where ß is the heating rate (°C/s).

The value of A and Ea are calculated using the least squares method. Sum of squared errors (SSE) is calculated using:

$$SSE = \sum[(X)_{calculated} - (X)_{data}]^2 \quad (9)$$

3. Results and Discussion

3.1 Characterization of SPR

The results of the ultimate analysis, protein, lipids, carbohydrates analysis and calculated higher heating value (HHV) of SPR are presented in Table 1. To investigate the potential of SPR as a promising energy source, each of these values is compared with *Chlorella vulgaris* with a high lipid content that has been extensively studied as a future source of energy.

The characteristics of SPR are similar to those of *Chlorella vulgaris*, particularly in C content (41.36-42.51 wt%), N content (6.66–7.17 wt%) and H content (6.60-6.77 wt%), but the content of O are slightly different. The O content in SPR (35.33%) is higher than in *Chlorella vulgaris* (27.95 wt%). In addition, the HHV of SPR is also higher (18.21 MJ/kg) when compared with *Chlorella vulgaris* (16.80 MJ/kg). This can be ascribed to the different C and O content. A larger C content and a smaller O content of the biomass will result in a greater HHV.

Table 1
The main characteristics of the SPR and *Chlorella vulgaris* (Ananda *et al*. 2016)

Component	SPR[a]	*Chlorella vulgaris*
Elemental analysis (wt%)		
Carbon	41.36	42.51
Hydrogen	6.60	6.77
Nitrogen	7.17	6.64
Oxygen	35.33	27.95
Higher heating value, HHV(MJ/kg)	18.21	18.80
Composition (dry-ash free, wt%)		
Protein	49.60	41.51
Lipid	0.01	15.71
Carbohydrate	25.60	20.99

[a]: This experiment

3.2 Thermogravimetric analysis

3.2.1 TG curves

The weight loss from thermal decomposition of SPR with 10, 20, 30, 40 and 50°C/min heating rates (HR), exhaled with 20 mL min^{-1} pure N_2 was studied. The TG curve for the heating rate of 20°C/min is shown in Figure 1. To understand the occurring process in the picture, the curve is divided into three stages. Stage I is water evaporation (30-230°C), Stage II (231-615°C) is pyrolysis, and Stage III is gasification (616-1000°C). The stage temperature obtained from TG curve is affected by the type and composition of biomass. For example, stage temperatures for *Chlorella vulgaris* with a heating rate 10°C/min are 50-180°C in Stage I, 181-615°C in Stage II, and 616-800°C in Stage III (Wang *et al*. 2016). In SPR pyrolysis, it can be seen that in Stage I for temperature 120-200°C, at 10.45-13.5 minutes, the curve forms a flat line because at 120°C the temperature is kept constant for 5 minutes. This is also the case at 600°C.

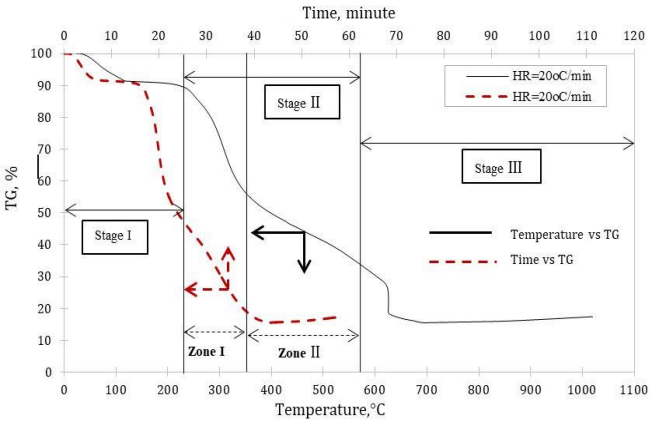

Fig. 1 Thermal decomposition of the SPR at heating rate 20°C/min

The thermal decomposition for the overall heating rate 10, 20, 30, 40 and 50°C/min is presented in Figure 2. As can be seen in Fig. 2, though the initial

temperature of pyrolysis begins to increase as the heating rate increases, the final temperature of the pyrolysis is not affected by the heating rate. This is due to the typical weight loss characteristics that will occur in each heating rate. The thermal decomposition of proteins and carbohydrates in the SPR is very complex, where there are simultaneous reactions between dehydration, depolymerization, re-polymerization, fragmentation, rearrangement and condensation. In case the time required for pyrolysis is greatly influenced by the magnitude of the heating rate, a greater heating rate results in a shorter pyrolysis time. The distribution of stage temperature range and time required for pyrolysis with heating rate 10, 20, 30, 40 and 50°C/min is listed in Table 2.

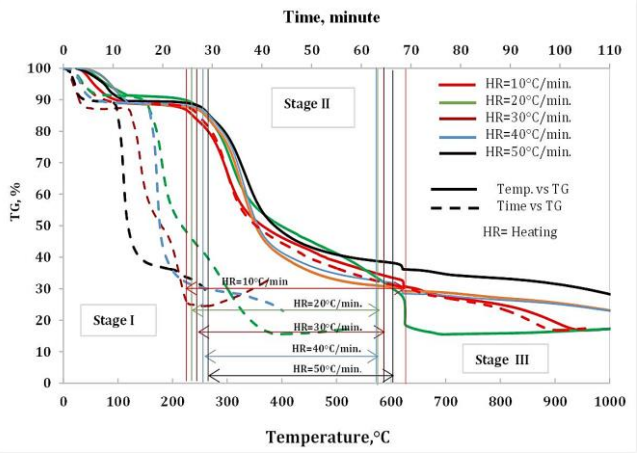

Fig. 2 Thermal decomposition at different heating rates

Table 2
Distribution of stage and time required for SPR pyrolysis at various heating rates

Heating rate, °C/min	10	20	30	40	50
Stage I, °C (Drying)	30–220	30–230	30–240	30–250	30–260
Stage II, °C (Pyrolysis)	221–615	231–570	241–585	251–570	261–600
Stage III, °C (Gasification)	616–1000	571–1000	586–1000	571–1000	601– 1000
Pyrolysis residence time, min	36.283	15.08	10.15	7.50	5.97

3.2.2 TG-DTA curves

Figure 3 depicts the TG-DTA curve at the heating rate 20°C/min. As it can be seen from Fig. 3 that the endothermic process occurs in Stage I with 2 low peaks at 79.37 and 116.34°C, with the heat requirement of 25.06 and 6.40 MW, respectively. Pyrolysis in Stage II is divided into 2 zones, i.e. zone 1 at 230-350°C and Zone 2 at 351-570°C. At this stage pyrolysis occurs exothermically with 3 strong peaks in Zone 2 at 378.32, 462.69 and 547.84°C, releasing 26.45, 40.45, and 47.64 MW of heat, respectively. At the top of the peak, the maximum heat dissipation occurs due to the decomposition of proteins and carbohydrates, where O-O, N-O, C-N, C-C, C-O, N-H, C- H, N = N, H = H, O-H, O = O, C = C, C = N, and C = O bonds are terminated. Since the SPR sample did not contain lipids, lipid decomposition did not occur. Following the pyrolysis is the gasification in Stage III occurring in endothermic condition, with 2 peaks at 632.64 and 689.16°C and heat requirement of 4.02 and 28.88 MW, respectively. As comparison, thermal decomposition of *Chlorella vulgaris* with 10°C/min heating rate produces one low endothermic peak in Stage I, one strong exothermic peak in Stage II, and one strong peak in Stage III (Wang *et al*. 2016). Differences in the number of peaks between SPR and *Chlorella vulgaris* can be due to differences in heating rate as well as the O, protein, carbohydrate and lipid content. It should be noted that the heat requirement for gasification will increase to 74 MW as the temperature rises up to 1000°C.

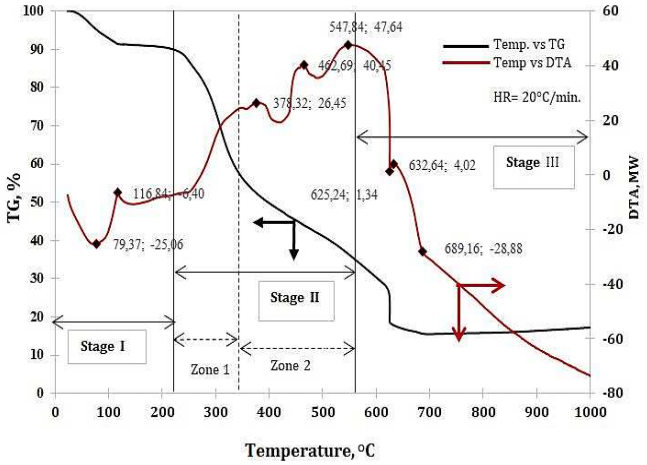

Fig. 3 TG-DTA curve at heating rate: 20°C/min

In Stage III, only non-condensable gases are released from char such as CO, CO_2, H_2 and CH_4 with very small weight loss. This may reflect that the heat required is relative only to the temperature rise, in which almost all volatile matter has been released in the pyrolysis zone. It is understandable because of the soft microalgae structure with relatively low lignin content (7.33 - 9.55 wt %), therefore volatile matter is easily removed from the tissues. Compared to hardwoods with large lignin content (25%) and complex tissues, the thermal decomposition in hardwood at above 600°C still produces non-condensable gas, explaining why its weight loss is relatively large (8-10%) (De Wild *et al*. 2011). To compare each peak in the overall heating rate tested, the same procedure at the

heating rate 20°C/min (Figure 3) was performed, resulting in the TG-DTA curve in Figure 4 and further listed in Table 4.

The division of the pyrolysis zone for other heating rates is done as in the heating rate of 20°C/min (Figure 3), where the distribution of pyrolysis zone for all heating rates is presented in Table 3.

Table 3
The distribution of SPR pyrolysis zone for various heating rates on SPR thermal decomposition.

Heating rate, °C/min	Zone 1	Zone 2
10	221–350	351-615
20	231–350	351-570
30	241-380	381-585
40	251–380	381-570
50	261-350	351–600

The peaks in DTA curves represent the events of heat increase, both endothermically and exothermically. In Stage II, pyrolysis for each heating rate of 10, 20 and 30°C/min produces 3 peaks at a certain temperature, slightly higher than the 2 peaks for the heating rate of 40 and 50°C/min. The difference in the number of peaks can be ascribed by the amount of heat flowed into the process in every minute. At the heating rate of 40 and 50°C/min, the heat is relatively large if compared to the heating rate of 10, 20 and 30°C/min. The heat requirement at these two heating rates is relatively sufficient for decomposition to occur at the beginning of pyrolysis, thus producing only 2 peaks. Furthermore, a positive peak value describes an exothermic process while a negative peak value describes an endothermic process. The endothermic and exothermic process occurs because of both the termination of low-energy bonding such as C-N, N-H, C-H of proteins as well as of high-energy bonding such as C=C, CH, C=N, C=O, OH and O=O which are commonly found in carbohydrates.

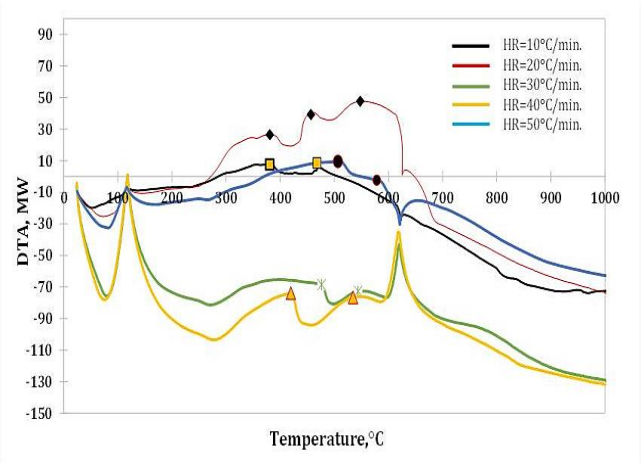

Fig. 4 The peaks on pyrolysis zone of DTA curve at the heating rate of 10, 20, 30, 40 and 50°C/min

Table 4
The peak on SPR pyrolysis zone and heat value for various heating rates

Heating rate, °C/min		10	20	30	40	50
Peak 1	Temp.°C	388.04	378.32	381.02	419.69	506.63
	DTA, MW	2.65	26.45	-65.48	-73.91	9.50
Peak 2	Temp.,°C	467.96	462.69	476.40	534.57	578.38
	DTA, MW	8.63	40.45	-68.48	-76.61	-2.34
Peak 3	Temp., °C	614.70	547.84	550.21	-	-
	DTA, MW	-20.79	47.64	-76.08	-	-

3.2.3 TG-DTG curves

The TG-DTG curve at the 50°C/min heating rate is presented in Figure 5, where each peak in Stage II signifies the release of volatile matter at certain temperature and rate of weight loss. The 2 peaks at Zone I in DTG curve occur at 267.48 and 331.05°C with the weight loss rate of 10.72 and 26.18 g/min, respectively. While protein and carbohydrate decomposition occurs in this zone, lipid decomposition does not take place due to the notably low lipid content in the SPR (0.01%wt). The second peak is the highest peak with a weight loss rate of 26.18 g/min at 331.05°C. Similar two peaks in Stage II were also obtained during thermal decomposition of *Chlorella vulgaris*, one peak in Zone I and one peak in Zone 2 (Wang *et al*. 2016).

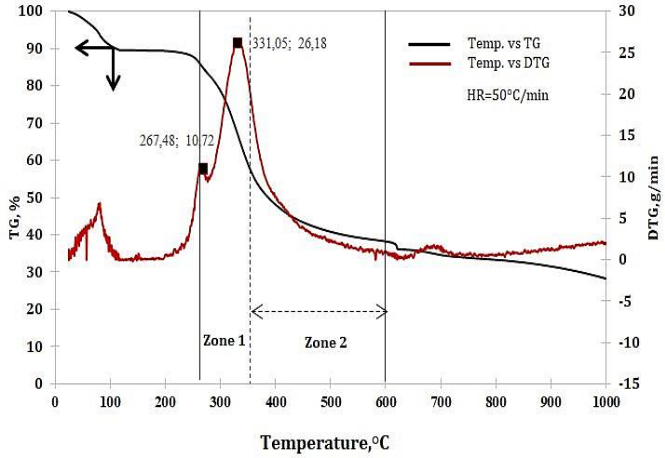

Fig. 5 TG-DTG curve at heating rate 50°C/min

The difference in peak temperature can be ascribed to the difference in heating rates as well as the composition of O content, protein, carbohydrate, and lipid. The peaks from DTG curve with the heating rate of 10, 20, 30, 40 and 50°C/min can be seen in Figure 6 and are listed in Table 5.

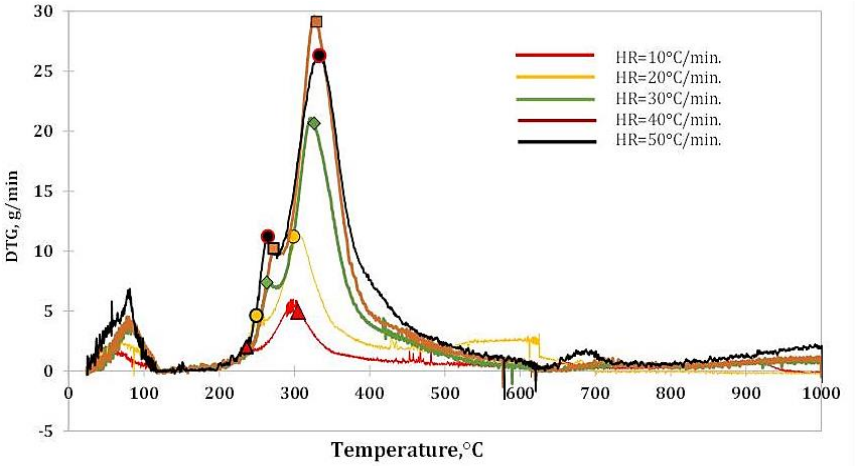

Fig. 6 The peaks on pyrolysis zone of DTG curve at the heating rate of 10, 20, 30, 40 and 50°C/min

Table 5
The peaks on DTG curve at various SPR pyrolysis heating rates

Heating rate, °C/min		10	20	30	40	50
Peak 1	Temp., °C	236.35 ± 2.36	249.12 ± 2.49	253.70 ± 0.54	272.15 ± 2.72	267.48± 2.67
	DTG, g/min	2.02 ± 0.02	4.64 ± 0.05	7.29 ± 0.07	10.22 ± 0.10	10.72 ± 0.11
Peak 2	Temp., °C	304.67 ± 3.04	288.45 ± 2.89	311.66 ± 3.12	329.47 ± 3.29	331.05 ± 3.31
	DTG, g/min	4.97 ± 0.05	11.10 ± 0.11	20.94 ± 0.21	29.12 ± 0.29	26.18 ± 0.26

Figure 6 illustrates the DTG curve for heating rate from 10 to 50°C/min. The rates of weight loss at each peak in the curve are listed in Table 5. The first peak at the lowest temperature occurs during the lowest heating rate (10°C/min) at 236.35°C with weight loss rate of 2.02 g/min. Furthermore, with the increase of the heating rate the first peak temperature also increases regularly, i.e., for heating rate of 20, 30, 40 and 50°C/min, the first peak occurs at 249.12, 253.70, 272.15 and 276.48°C, respectively. It is deduced that the increase of the heating rate does not affect the temperature of the second peak, as it is seen that the temperature at the second peak fluctuates. Although the initial temperature peak appears to rise regularly with the increase of heating rate, the increase of heating rate actually results in shorter initial peak, i.e., for heating rate 10, 20, 30, 40 and 50°C/min, the first peak occurs in 27.17, 17.33, 19.1, 17.67, and 11 minutes. From the five tested heating rates, the highest peak found occurs during the heating rate 40°C/min at 329.47°C with a weight loss rate of 29.12 g/min. It is at this peak that the most rapid and large volatile matter release occurred, resulting in a large heat requirement.

3.3 Kinetics

The reaction kinetic for the one-step global model can be derived from Equation (3), where the value of collision factor (A) and activation energy (Ea) can be calculated using Equations (5)–(8) with SSE calculation in Matlab using Equation (9). The calculated values of A, Ea, and k for each heating rate in Zone 1 are presented in Table 6 and Zone 2 in Table 7. Equation 7 is evaluated, where the pyrolysis temperature (T) is influenced by heating rate (ß) and time (t). The relationship between pyrolysis time and temperature ($(T)_{calculated}$ and $(T)_{data}$) in Zone 1 and 2 are presented in Fig. 7. For both zones, it can be seen that the $(T)_{calculated}$ and $(T)_{data}$ value coincide with one another.

Furthermore, the calculated conversion $(X)_{calculated}$ from Eq. (6) and the conversion observed from the experiment $(X)_{data}$ are employed to calculate Sum of squared errors (SSE). The relationship of both of these conversions with time can be seen in Fig. 8. In Fig. 7 and 8, the heating rate of 20°C/min is selected because it produces the smallest SSE value of 0.0506 for Zone 1 and 0.0427 for Zone 2. The SSE values between $(X)_{calculated}$ and $(X)_{data}$ indicate that one-step global

model can be used for the calculation of Ea and k at a certain temperature range. The SSE value for the other heating rates (10, 30, 40 and 50°C/min) was investigated in the same way as the heating rate of 20°C/min, and the results are set forth in Table 6 and Table 7. It appears that the SSE value for all heating rates is relatively small.

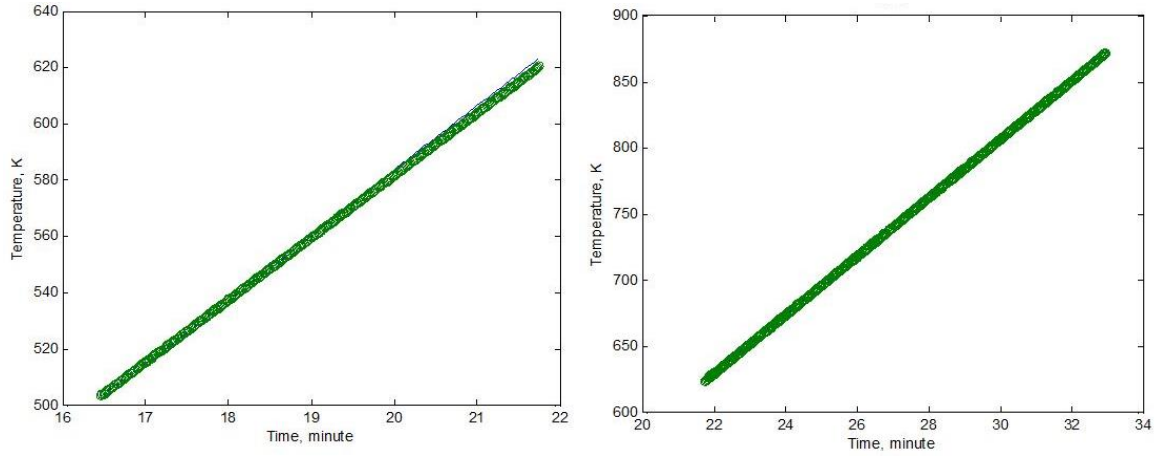

(7a) (7b)

Fig. 7 The relationship between time and pyrolysis temperature for heating rate of 20°C/min in (a) Zone 1 and (b) Zone 2

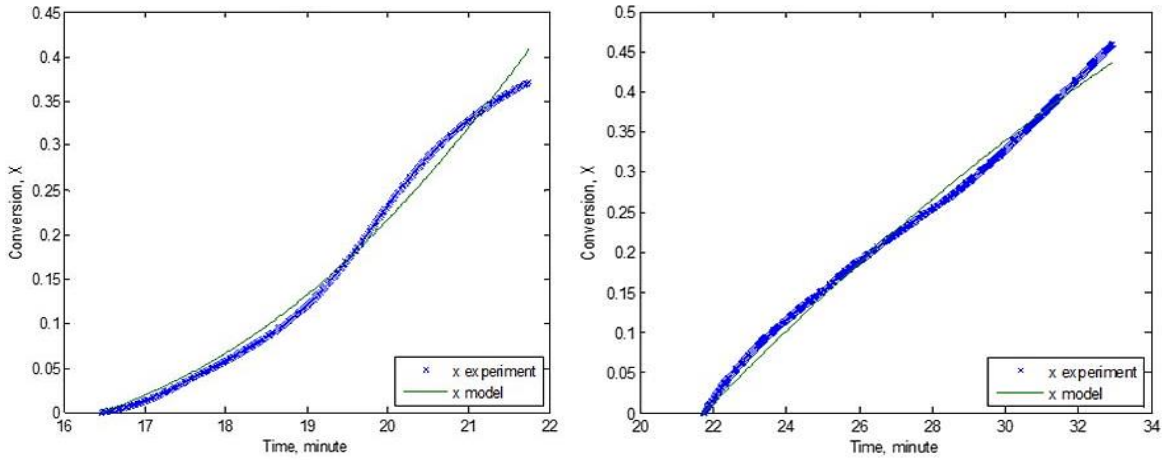

(8a) (8b)

Fig. 8 The relationship between time and conversion for heating rate of 20°C/min in (a) Zone 1; (b) Zone 2

The calculation results for all heating rate show that the increase in heating rate affects the value of Ea and A. The pyrolysis temperature range of each heating rate is not similar, possibly due to typical SPR characteristics when pyrolysis involves a very complex reaction simultaneously.

The global one-step model equation applies only to a certain temperature range and can not be used for the overall pyrolysis temperature range. It is necessary to divide the pyrolysis zone by looking at the tendency of TG curve or weight loss curve. Figure 9 shows the relation between the rate of reaction constants (k) and reaction temperature at various heating rates in Zone 1 and Zone 2. The slope of the TG curve in Zone 1 is very steep for all heating rates.

From Table 6 it can be deduced that for heating rate 10, 20, 30, 40 and 50°C/min with the reaction order n=1, activation energy (E_a) value tends to increase with the increase of heating rate. A higher heating rate value will promote a higher A value, hence increasing Ea as well. The A and Ea value increase regularly but start to be constant as it reaches the heating rate of 40-50 ° C/min. Thus, the recommended heating rate for the optimum plant design is at 40-50°C/min. Furthermore, it can be concluded from SPR pyrolysis results that with the heating rate 10-50°C/min, Ea for protein and carbohydrate decomposition lies within 35.46-47.89 KJ/mol with reaction rate constant (k) value lies in the range of (0.0168-0.1021) - (0.0995-0.4691) sec^{-1}. The value of Arrhenius (A) factor, Ea and k for various heating rate in Zone 2 are presented in Table 7.

Table 6
Reaction kinetic parameters of the SPR for Zone I

Heating rate, °C/min	A	Ea [J/mole]	SSE	Temperature range [K]		k [sec^{-1}] low temp	k [sec^{-1}] high temp
10	95.86±0.96	35,454.53±354.54	0.1870	220 ±2.2	350±3.5	0.0168±1.7x10^{-4}	0.1021±1.0x10^{-3}
20	593.30±5.93	41,101.53±411.02	0.0506	230 ±2.3	350±3.5	0.0319±3.2x10^{-4}	0.2123±2.1x10^{-3}
30	2,218.43±22.18	45,702.05±457.02	0.1155	240±2.4	380±3.8	0.0493±5.0x10^{-4}	0.4899±4.9x10^{-3}
40	4,607.19±46.07	47,892.37±478.92	0.0651	250±2.5	380±3.8	0.0759±7.6x10^{-4}	0.6797±6.8x10^{-3}
50	4,562.70±45.63	47,562.27±475.62	0.6524	260±2.6	350±3.5	0.0995±1.0x10^{-3}	0.4691±4.7x10^{-3}

Tabel 7
Reaction kinetic parameters of the SPR for Zone 2

Heating, rate °C/min	A	Ea, J/mole	SSE	Temperature range [K]		k [sec^{-1}] low temp.	k [sec^{-1}] high temp.
10	0.0204±2x10^{-4}	0.1428±1.4x10^{-3}	0.3472	351±3.5	615±6.2	0.0203±2x10^{-4}	0.0203±2x10^{-4}
20	0.0489±5x10^{-4}	0.1240±1.2x10^{-3}	0.0427	351±3.5	570±5.7	0.0489±4.9x10^{-4}	0.0489±4.9x10^{-4}
30	0.0693±7x10^{-4}	0.0179±1.8x10^{-3}	0.3389	381±3.8	585±5.9	0.0693±6.9x10^{-4}	0.0693±6.9x10^{-4}
40	0.1321±1x10^{-4}	0.0100±1x10^{-3}	0.9220	381±3.8	570±5.7	0.1321±1.3x10^{-3}	0.1321±1.3x10^{-3}
50	0.1278±1x10^{-4}	0.0096±1x10^{-4}	0.8811	351±3.5	600±6	0.1278±1.3x10^{-3}	0.1278±1.3x10^{-3}

From Table 7 it appears that the A value is relatively small and rises regularly with an increase in the heating rate to 40°C/min. On the other hand, Ea value decreases regularly with the increase of heating rate. This indicates that in Zone 2 the release of volatile matter is not as large as in Zone 1, as it is characterised by weight loss rate with peaks appearing only in Zone 1. This is different from zone 2 where pyrolysis is stable with the slope of the TG curve tends to be flat. The activation energy for heating rate 10, 20, 30, 40 and 50°C/min respectively is 0.0001428, 0.0001240, 0.0000179, 0.0000100 and 0.0000096 KJ/mol, while the k value is 0.0204, 0.00489, 0.0693, 0.1321 and 0.1278 sec^{-1}, respectively.

The effect of the heating rate on the value of k for zone 1 and zone 2 is shown in Figure 9. It is seen that in Zone 1 for each heating rate, the k value increases sharply along with the rise in temperature, where it is influenced by temperature, Ea and A. For zone 2 on various heating rate, the effect of temperature rise to k is relatively small as the k value for each heating rate is constant, as depicted in Fig. 9 with a flat line.

At the same heating rate of 10 °C/min, the Ea value of SPR pyrolysis (35.45 kJ/mol) in Zone 1 and (0.0001428 kJ/mol) in Zone 2 are much lower than the Ea value for *Chlorella vulgaris* both in Zone I (51 KJ/mol) and Zone 2 (1.64 KJ/mol) in Zone 2. The significant difference in Ea in Zone 1 is due to the different protein, carbohydrate and lipid contents. Whereas in Zone 2, the very small Ea value for SPR indicates that there is no lipid decomposition because of its very small lipid content (0.01 wt.%). This is different for Zone 2 for *Chlorella vulgaris*, where the Ea value of 1.64 KJ/mol indicates that lipid decomposition still occurs in Zone 2.

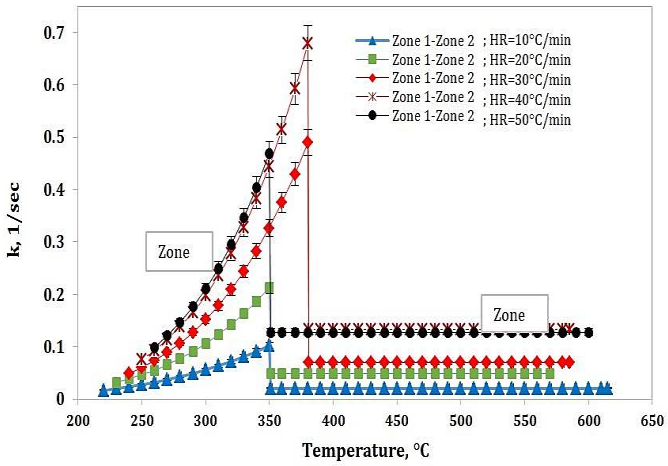

Fig. 9 The relation between the rate of reaction constants (k) and reaction temperature at various heating rates in Zone 1 and Zone 2

4. Conclusion

Spirulina platensis residue (SPR) with a high protein and carbohydrate content exhibits the potential to be processed into an energy source with pyrolysis. However, it is necessary to understand the thermal decomposition and kinetics data of the pyrolysis for the reactor design. In this work, a TG-DTA-DTG analysis has been developed to investigate the characteristics of

pyrolysis, activation energy (Ea) and reaction rate constant (k) for each heating rate. One step global model is suitable for all heating rate at certain temperature range for zone 1 and 2. In Zone 1, the bigger the heating rate the bigger Ea and k values, whereas for zone 2 the bigger the heating rate the smaller the Ea and k value. Thermal decomposition in Stage I occurs in endothermic condition. On the other hand, in Stage II thermal decomposition is exothermic for heating rate 10, 20 and 50°C/min and endothermic for the heating rate of 30 and 40°C/min. The gasification process occurs in Stage III in endothermic condition. From the DTA curve, 3 peaks were obtained for heating rates 10, 20 and 30°C/min and 2 peaks for heating rates 40 and 50°C/min in the pyrolysis zone. For all heating rate, 2 peaks were obtained from DTG curve at zone 1 with the highest peak found for heating rate 40 °C/min, i.e. at 329.47°C with weight loss rate of 29.12 g/min.

Acknowledgments

The authors gratefully thank Faith and the Directorate General of Higher Education, Ministry of Research Technology and Higher Education, the Republic of Indonesia for the support and funding in the scheme of "International Research Collaboration and Scientific Publication" under the supervision of Research Institutions and Community Service, Gadjah Mada University, Yogyakarta, Indonesia. The authors are also thankful for Muhamad Hartono and Takdir for his help during the manuscript preparation.

References

Agrawal, A. & Chakraborty, S. (2013) A kinetic study of pyrolysis and combustion of microalgae *Chlorella vulgaris* using thermo-gravimetric analysis. *Bioresour. Technol.*, 128, 72–80.

Ananda, V., Sunjeeva, V. & Vinua, R. (2016) Catalytic fast pyrolysis of *Arthrospira platensis* (spirulina) algae using zeolites. *J. Anal. Appl. Pyrolysis*, 118, 298–307.

Chisti, Y. (2008) Biodiesel from microalgae beats bioethanol. Trends. *Biotechnol.*, 26, 126 - 131. doi:10.1016/j.tibtech.2007.12.002.

Chaiwong, K., Kiatsiriroat, T., Vorayos, N. & Thararax, C. (2013) Study of bio-oil and bio-char production from algae by slow pyrolysis. *Biomass Bioenerg.*, 56, 600-606.

Ceylan, S., Topcu, Y. & Ceylan, Z. (2014) Thermal behaviour and kinetics of algae *Polysiphonia elongata* biomass during pyrolysis. *Bioresour. Technol.*, 171, 193–198.

Chen, W.H., Lin, B-J., Huang, M-Y. & Chang, J-S. (2015) Thermochemical conversion of microalgal biomass into biofuels: A review. *Bioresour. Technol.*, 184, 314–327.

Dragone, G., Fernandes, B., Vicente, A. & Teixeira, J.A. (2010) Third generation biofuels from microalgae. In: Vilas AM, editor. Current research, technology and education topics in applied microbiology and microbial biotechnology. Badajoz: Formatex Research Center; 1355-66.

De Wild, P.J., Reith, H. & Heeres, H.J. (2011) Biomass pyrolysis for chemicals. Biofuels, 2 (2), 185 – 208.

Daniyanto, Sutijan, Deendarlianto, & Budiman, A. (2016) Reaction kinetic of pyrolysis in mechanism of pyrolysis-gasification process of dry torrified-sugarcane bagasse. ARPN *Journal of Engineering and Applied Sciences*, 11, Issue 16, 9974-9980.

El-Sayed, S.A. & Mostafa, M.E. (2014) Pyrolysis characteristics and kinetic parameters determination of biomass fuel powders by differential thermal gravimetric analysis (TGA/DTG). *Energ. Conversion and Manag*, 85, 165–172.

Hadiyanto, Widayat & Kumoro, A.C. (2012) Potency of microalgae as biodiesel source in Indonesia. Int. *Journal of Renewable Energy Development*, 1, 23-27.

Hadiyanto H., Christwardana, M. & Soetri, D. (2013) Phytoremediations of palm oil mill effluent (POME) by using aquatic plants and microalgae for biomass production. Journal of Environmental and Technology. ISSN 1994-7887/DOI:10.3923/jest.2013.

Hu, M., Chen, Z., Guo, D., Liu, C., Xiao, B., Hu, Z. & Liu, S. (2015) Thermogravimetric study on pyrolysis kinetics of *Chlorella pyrenoidosa* and bloom-forming cyanobacteria. *Bioresour Technol.*, 177, 41–50.

Lia, J., Wanga, G., Wanga, Z., Zhanga, L., Wang, C. & Yang, Z. (2013) Conversion of *Enteromorpha prolifera* to high-quality liquid oil viadeoxy-liquefaction. *J. Anal. Appl. Pyrolysis*, 104, 494–501.

Li, S., Ma, X., Liu, G. & Guo, M. (2016) A TG–FTIR investigation to the co-pyrolysis of oil shale with coal. *J. Anal. Appl. Pyrolysis*, 120, 540–548.

Ojolo, S.J., Oshekub, C.A. & Sobamowoa, M.G. (2013) Analytical investigations of kinetic and heat transfer in slow pyrolysis of a biomass particle. *Int. Journal of Renewable Energy Development*, 2 (2), 105-115.

Prakash, N. & Karunanithi, T. (2008) Kinetic modeling in biomass pyrolysis – A Review. *J. Appl. Sci. Res.*, 4(12), 1627-1636.

Pratama, N.N. & Saptoadi, H. (2014) Characteristics of waste plastics pyrolytic oil and its applications as alternative fuel on our cylinder diesel engines. *Int. Journal of Renewable Energy Development*, 3 (1), 13-20

Sunarno, Herman, S., Rochmadi, Mulyono, P. & Budiman, A. (2017) Effect of Support on Catalytic Cracking of Bio-Oil over Ni/Silica-Alumina. AIP Conference Proceedings 1823, 020089; doi: 10.1063/1.4978162.

Suganya, T., Varman, M., Masjuki, H.H. & Renganathan, S. (2016) Macroalgae and microalgae as a potential source for commercial applications along with biofuels production: A biorefinery approach. *Renew Sust Energ Rev*, 55, 909–941.

Wijffels, R.H., Barbosa, M.J. & Eppink, M.H.M. (2010) Microalgae for the production of bulk chemicals and biofuels. *Biofuels Bioproducts & Biorefining-Biofpr*. 4(3), 287-295.

Widiyannita, A.M., Cahyono, R.B., Budiman, Sutijan, A. & Akiyama, T. (2015) Study of pyrolysis of ulin wood residues. AIP Conference Proceedings 1755, 050004.

Wang, X., Hu, M., Hu, W., Chen, Z., Liu, S., Hu, Z. & Xiao, B. (2016) Thermogravimetric kinetic study of agricultural residue biomass pyrolysis based on combined kinetics. *Bioresour. Technol.*, 219, 510–52.

Wicakso, D.R., Sutijan, Rochmadi, & Budiman, A. (2017) Study of catalytic upgrading of biomass tars using Indonesian iron ore. AIP Conference Proceedings 1823, 020094; doi: 10.1063/1.4978167